HHS Public Access

Author manuscript

Pharm Res. Author manuscript; available in PMC 2020 May 04.

Published in final edited form as:

Pharm Res. ; 35(11): 203. doi:10.1007/s11095-018-2483-5.

Modeling Sex Differences in Anti-inflammatory Effects of Dexamethasone in Arthritic Rats

Dawei Song[1], **Debra C. DuBois**[1,2], **Richard R. Almon**[1,2], **William J. Jusko**[1]

[1]Department of Pharmaceutical Sciences, School of Pharmacy and Pharmaceutical Sciences, State University of New York at Buffalo, Buffalo, New York 14214, USA

[2]Department of Biological Sciences, State University of New York at Buffalo, Buffalo, New York 14260, USA

Abstract

Purpose—Collagen-induced arthritic (CIA) rats are used commonly for preclinical pharmacologic research into rheumatoid arthritis (RA). Dexamethasone (DEX), a potent corticosteroid (CS), remains an important component in combination therapy for RA. Although sex differences in RA and CS pharmacokinetics/pharmacodynamics (PK/PD) have been documented in humans, there has been no such comprehensive evaluation of sex differences in CIA rats.

Methods—Paw size measurements were obtained for males and females from four groups of animals: healthy controls, non-drug treated arthritic animals, and both 0.225 and 2.25 mg/kg DEX-treated arthritic animals. A turnover model for disease progression, minimal PBPK model for drug concentrations, and inhibitory indirect response model were applied using population PK/PD modeling.

Results—The clearances of DEX were 43% greater in males, but other PK parameters were similar. The temporal profiles of paw swelling exhibited earlier progression, peak edema times, and disease remission in females. DEX suppressed paw edema well in both males and females with similar capacity (I_{max}) values (=1.0), but DEX potency was less in females with higher IC_{50} values (0.101 *versus* 0.015 ng/mL).

Conclusions—The pharmacology of DEX was well characterized in CIA rats. This study addresses knowledge gaps about sex differences and can be a guide for more mechanistic assessment of sex, drug, and disease differences in RA.

Keywords

collagen-induced arthritis; dexamethasone; pharmacodynamics; pharmacokinetics; sex differences

INTRODUCTION

Rheumatoid arthritis (RA) is a common inflammatory auto-immune disease affecting 0.5–1.0% of the adult population in developed countries with an approximately two-fold greater

William J. Jusko, wjjusko@buffalo.edu.

occurrence in women [1]. The disease produces pain, stiffness and edema of joints, cartilage degradation, and bone erosion, which are associated with continuous synovitis and systemic and local levels of inflammation and autoantibody production [1]. RA primarily targets synovial tissues, which results in permanent joint damage and potential disability [1,2]. The major cause is the production of pro-inflammatory mediators including cytokines, chemokines and prostaglandins secreted by activated immune and other relevant cells [3,4]. Current treatment options for RA include rapid-acting nonsteroidal anti-inflammatory drugs (NSAIDs), corticosteroids (CS), slow-acting disease-modifying drugs (DMARDs) such as methotrexate, and biologics such as infliximab [2,5].

DEX, a clinically used therapeutic CS, exhibits potent anti-inflammatory and immunosuppressive properties. DEX binds to cytosolic glucocorticoid receptors and after CS/GR translocation into the nucleus inhibits nuclear factor κB (NF-κB), activator protein-1 (AP-1) and MAPK signaling. This inhibition diminishes the production and biological/pathological effects of downstream pro-inflammatory mediators, including tumor necrosis factor (TNF)-α, interleukin (IL)-1β, and IL-6, resulting in a dampening of immunological functions [6,7]. In addition, non-genomic interactions of DEX with signaling molecules and membrane-associated receptors may contribute to its rapid therapeutic effects [8,9].

Although sex differences in the prevalence, disease risk factors and progression as well as prognosis in RA patients have been documented [10–12], exploration of underlying mechanisms is needed [13,14]. Sex differences in corticosteroid PK/PD have been found in healthy subjects [15] and sex differences in human or murine immune systems have been reviewed [11,16,17] The CIA rat and mouse models are commonly used in preclinical RA research for physiological and pharmacological evaluation [18–21].

A small-scale PK/PD/disease (DIS) systems model was developed to assess DEX effects on paw edema at the transcriptional level in male CIA rats, but female rats were not included [21–23]. Female CIA rats may show a different timeline of disease progression and different temporal profiles of major pro-inflammatory cytokines [24,25]. The purpose of the current study is to compare disease progression and DEX pharmacokinetics/pharmacodynamics (PK/PD) in female and male CIA rats.

MATERIALS AND METHODS

Reagents and Chemicals

Dexamethasone sodium phosphate solution (pharmaceutical grade) was purchased from Bimeda Pharmaceuticals (Dublin, Ireland). Type II porcine collagen was supplied by Chondrex Inc. (Redmond, WA). Incomplete Freund's adjuvant (IFA) and all other chemicals were purchased from Sigma-Aldrich (St Louis, MO).

Animals

Male and female Lewis rats were purchased at 5–6 weeks from Envigo (Indianapolis, IN) with initial body weights around 160 g (males) and 120 g (females). All rats were housed individually with free access to food and water in the University Laboratory Animal Facility and acclimated for 7 days before experimentation. The study design and research protocol

followed the *Guide for the Care and Use of Laboratory Animals* (National Research Council, 2011) and were approved by the University at Buffalo Institutional Animal Care and Use Committee.

Experimental Design/Procedures

Studies involved four groups of animals: healthy controls to assess natural growth, non-drug treated arthritic animals to assess disease progression, and 0.225 and 2.25 mg/kg DEX-treated arthritic animals. Animal manipulations (arthritis induction, daily paw measurements, and drug administration) were carried out between 8 and 10 AM, which corresponds to a time at which endogenous corticosterone is at its nadir. The induction of CIA using porcine collagen injected intradermally in IFA was described in detail in a previous publication from our lab [21]. Edema of the hind paw was evaluated by measuring cross-sectional areas of the forefoot and the ankle by digital calipers (VWR Scientific, Rochester, NY). A pilot study showed that paw edema peaked on day 16 post-induction for females and on day 21 for males. Paw measurements were therefore performed every 2–3 days immediately after induction, and more frequently after swelling became significant (day 11 for females and day 17 for males). Disease penetrance was approximately 60% for males and 80% for females. Therefore, paw edema evaluated on day 15 for female rats and day 20 for male rats was used as selection criteria for successful arthritis induction: only rats with at least a 50% increase in at least one hind paw were selected for inclusion in studies. For DEX treated animals, a single dose of drug was administered at peak edema: day 16 for females and day 21 for males. The DEX dosing solution was prepared fresh through dilution with phosphate-buffered saline (PBS) to achieve final concentrations of 0.225 or 2.25 mg/ml. DEX was injected subcutaneously (SC) at the nape of the neck with injection volumes of 1 ml/kg. For DEX PD studies, paw edema was further assessed at 1, 2, 4, 6, 8, 12, 24, 36, 48 h post-dosing and then daily for an additional 7 days. For PK studies, serial blood sampling from the saphenous vein was performed on 3–4 rats per dose group. Details for blood sampling, plasma processing, and LC/MS assay for plasma DEX were described previously [26].

PK/PD Models

DEX PK Modeling and Simulation—The basic mPBPK model shown in Fig. 1 [27] was employed to characterize the plasma DEX concentration-time profiles. Detailed model descriptions and assumptions are provided by Li et al. [26].

The mathematical equations and initial conditions:

$$\frac{dA_a}{dt} = -k_a \cdot A_a, A_a(0) = \text{Dose}_D \cdot F \tag{1}$$

$$\frac{dC_p}{dt} = \left[k_a \cdot A_a + f_d \cdot Q_{co} \cdot \left(\frac{C_t}{K_p} - C_p\right) - CL_p \cdot C_p\right]/V_p, C_p(0) = 0 \tag{2}$$

$$\frac{dC_t}{dt} = \left[f_d \cdot Q_{co} \cdot \left(C_p - \frac{C_t}{K_p} \right) \right] / V_t, C_t(0) = 0 \quad (3)$$

with physiological restrictions of $f_d \leq 1$ and $V_p + V_t$ = Body weight, where A_a indicates the amount of DEX at the absorption site, k_a represents the first-order absorption rate constant, C_p and C_t are total DEX concentrations in V_p and V_t (plasma and tissue volumes), K_p is the tissue/plasma partition coefficient, f_d is the fraction of drug in Q_{co} entering V_t, CL_p is the systemic clearance, and F is the bioavailability of DEX (0.86) in rats [28,29].

The PK parameters of DEX were previously obtained by using this model to fit DEX plasma profiles in healthy male and female rats after 2.25 mg/kg dosing [26] and the model was used to simulate total tissue concentrations of DEX (C_t) in arthritic rats receiving 0.225 and 2.25 mg/kg DEX, based on dose linearity and no influence from inflammation in CIA rats [28,29]. The unbound fraction of DEX in interstitial fluid (ISF) (f_{uISF}) was calculated from:

$$f_{uISF} = \frac{1}{1 + (E/P)(1 - f_{up})/f_{up}} \quad (4)$$

where E/P is the ratio of protein concentrations in ISF and plasma [30] and 0.9 was used for arthritic rats as described previously [26]. Unbound DEX concentrations in ISF (C_{uISF}) were calculated from $C_{uISF} = C_t \cdot f_{uISF}$. Parameter values used for PK simulations are listed in Table I.

DEX Pharmacodynamics—The PD model shown in Fig. 1 was utilized to characterize disease (DIS) progression in CIA rats, as well as anti-inflammatory effects of DEX. Detailed model description and assumptions are the same as in Li *et al.* [26].

The mathematical equations, and initial conditions are:

Natural growth of paw in all groups before disease onset:

$$\frac{dPaw}{dt} = k_g \cdot Paw \cdot \left(1 - \frac{Paw}{Paw_{ss}} \right), t < t_{onset} Paw(0) = Paw^0 \quad (5)$$

After disease onset, disease progression in CIA rats without DEX treatment are

$$\frac{dPaw}{dt} = k_g \cdot Paw \cdot \left(1 - \frac{Paw}{Paw_{ss}} \right) + k_{in}(t) - k_{out} \cdot Paw, t \geq t_{onset} Paw(0) = Paw^0 \quad (6)$$

$$\frac{dk_{in}}{dt} = -k_{dg} \cdot k_{in}, k_{in}(0) = k_{in}^0 \quad (7)$$

For DEX-treated CIA rats, drug effects were modeled mechanism-based indirect response model I (IDR I) to count for the inhibition of DEX on paw swelling [31,32].

$$\frac{dPaw}{dt} = k_g \cdot Paw \cdot \left(1 - \frac{Paw}{Paw_{ss}}\right) + k_{in}(t) \cdot \left(1 - \frac{I_{max} \cdot C}{IC_{50} + C}\right) - k_{out} \cdot Paw, t \geq t_{onset} Paw(0) = Paw^0 \quad (8)$$

where Paw is paw size measurements obtained by digital calipers; Paw_0 is the paw size at the beginning of the study; Paw_{ss} is the paw size at steady-state following logistic natural growth; k_g is the first-order growth rate constant of paw size in healthy rats; t_{onset} is the time when disease progression is reflected by paw size; $k_{in}(t)$ represents the production rate of paw edema after disease onset as a function of time; k_{deg} is a first-order rate constant in the k_{in} function accounting for the observed remission of CIA; k_{out} is the first-order rate constant for the loss of edema; I_{max} is the maximum inhibitory effect of DEX on production of paw edema and IC_{50} is the unbound ISF concentration (C_{uISF}) of DEX required for 50% of maximal effect.

Model Fitting—The PK parameter estimates were fixed for concentration-time profiles simulations in the PD analysis in CIA rats (Table I). Data for male CIA rats from previous studies were also used in model development [21,23]. Population PK/PD modeling was performed using the first-order conditional estimation with interaction (FOCE-I) implemented in NONMEM 7.3 [33]. NONMEM was utilized with Perl-speaks-NONMEM (PsN, version 4.7.0), Xpose (version 4), Pirana (version 2.9.6) [34,35] and data manipulation and plotting were done using R (version 3.4.3) [36] and SigmaPlot (version 12.5, Systat Software, San Jose, CA). The inter-individual variability (IIV) was modeled with an exponential form and proportional function was used for residual variability (RV) modeling. The addition of fixed and random effect parameters was determined when successful minimization and a decrease of 3.84 (a commonly used threshold in population analysis) in the objective function value (OFV) was achieved ($P< 0.05$, df = 1) when Chi-squared distribution reflects statistical significance. Backward elimination of parameters with dOFV smaller than 10.83 ($P < 0.001$, df = 1) was conducted. The final model was evaluated based on the objective function, diagnostic plots, and precision of parameter estimates.

RESULTS

PK/PD of DEX in CIA Rats

Plasma DEX concentrations after 2.25 mg/kg DEX dosing in healthy male and female rats and simulated tissue concentration-time profiles of DEX in CIA rats for 2.25 and 0.225 mg/kg doses as well as calculated unbound ISF concentration are shown in Fig. 2. The simulated DEX profiles were comparable to previous results [26]. The unbound ISF concentrations of DEX were used to control drug effects in the PD model as only unbound DEX is assumed to penetrate cell membranes and bind to GR mediating its immunosuppressive properties. The simulated ISF free DEX area under the curve (AUC) from 0 to 24 h at 2.25 mg/kg dosing was 2809 for female and 1968 ng·h/mL for male CIA rats. For 0.225 mg/kg dosing, corresponding AUC values were 281 and 197 ng·h/mL.

DEX was administered on day 16 for females and day 21 for males after induction, because paw edema peaked at these times and we wished to explore drug PK/PD when symptoms

were maximal. There were 532 rats with 5380 observations in the four subgroups: healthy control, vehicle-control CIA rats, 0.225 mg/kg dosed CIA rats, 2.25 mg/kg dosed CIA rats for both males and females with approximately a 1:1 sex ratio in terms of observation numbers. Figure 3 compares PD profiles across different subgroups and between the sexes. Natural growth can be observed for CIA groups before disease onset. After DEX dosing, paw edema was rapidly suppressed, and drug effects can last for 2–3 days. In non-dosed CIA animals, natural remission of disease can be observed at later times. Generally, disease onset and remission occurred earlier in female CIA animals than males. A naïve-pooling approach was first applied in order to obtain initial parameter estimates used in the following population analysis. Population modeling started with the base model shown in Fig. 1 and two parameters (Paw_0, Paw_{ss}) were recognized as structural components based on the paw size differences between female and male rats in the beginning of the study and after entering the natural growth plateau. Then added IIV was tested for each PD parameter with an assumption that IIV was similar in males and females in order to avoid over-parameterization. The available data were not informative enough to support the identification of Eta for more than two parameters. Therefore, we estimated IIV for two parameters (k_{in}^0, Paw_0).

For covariate analysis, forward selection was conducted first. The necessity for sex specificity of three parameters (k_g, k_{out} and Imax) was ruled out, but covariate effects of sex on the other four parameters (k_{in}^0, k_{deg}, $Tonset$ and $IC50$) were found to be significant (dOFV >3.84). In addition, the I_{max} for males and females were both estimated to be 0.999, so both were fixed to 1. Then stepwise backward elimination was employed to refine the model. Elimination of sex for only one parameter (k_{in}^0) did not result in significantly increased OFVs, so sex effects on the other three parameters (k_{deg}, $Tonset$ and $IC50$) were retained in the final assessment.

The final model estimates are shown in Table II. Parameter estimates with reasonable precisions were obtained after NONMEM fitting, but the RSE for male IC_{50} was somewhat higher. For three shared parameters (k_{in}^0, k_g, k_{out}), estimates were comparable to those from a previous study [26]. For k_g, a value of 0.0010 (1/h) was found, near to a value of 0.0020 (1/h) as obtained for both sexes previously. Similarly, k_{out} equaled 0.0088 (1/h) somewhat smaller than values of 0.015 and 0.012 (1/h) for females and males obtained previously. Furthermore, k_{in}^0 was 1.66 (1/h) near to previous values 2.18/1.72 (1/h). The steady-state paw sizes (Paw_{ss}) in the current model were 73.1 and 108 (mm^2), which was consistent with the larger body size of male animals. The T_{onset} was estimated to be 256 h (female) and 300 h (male) similar to reported values from several studies [21,26,37] and reflects the reproducibility of disease progression in both female and male CIA models. In the current study, the IIV tended to characterize the variability among batches of rats successfully instead of giving different initial values of k_{in}^0 and $Paw0$ for different subgroups. For paw size on day 0, females had an estimate of 57.1 mm^2 and males 78.1 mm^2 similar to reported values [26], consistent with male rats being larger. Unexpectedly, the k_{deg} estimate for females was greater (0.00099 *versus* 0.00047 mm^2/h), which was estimated jointly in our previous study [26]. For drug efficacy, IC_{50} values were 0.101 ng/mL in females and 0.0146

ng/mL in males, which was reflected by strong inhibition of paw edema after DEX injection even at low doses and suggested less efficacy in female CIA rats. Because the male IC_{50} was estimated with high RSE, careful assessment is necessary before accepting the result. Population predicted paw sizes for each group are shown in Fig. 4 showing the size and DEX efficacy differences. Figure 5 shows the goodness of fit plot for the final model estimation. The upper panel shows good agreement between population predictions/ individual predictions and observed data. Symmetrical and even distributions around zero can be seen in both plots. Therefore, the general model structure and residual variability equation are appropriate for characterizing the currently available data.

DISCUSSION

The CIA rat model is one of the most frequently adopted preclinical disease animal models, serving as a surrogate to investigate the biological mechanisms of human RA [18]. DEX, like many other potent synthetic CS, remains an important component in combination therapy for RA. Carefully-controlled animal studies and comprehensive evaluation of disease endpoints allow the development of mechanistic mathematical models to reflect endogenous biological processes and their perturbations in inflammation due to the induction of CIA and dosing of DEX. The current study attains DEX concentrations that are similar to human exposures and extends our previous assessments in male rats [21–23,26,29] to characterize disease progression and DEX effects on paw edema in female and male CIA rats to explore sex differences through symptom observations and PD parameter comparisons. Model parameters are generally similar with previous results considering the much larger data base employed here and use of population rather than naïve pooling approaches.

The PK model in our study was applied to characterize DEX in healthy male and female rats and showed different systemic clearances [26]. DEX is extensively metabolized by cytochrome P450 (CYP) 3A family members in both humans and rats [38]. A previous study showed a significant increase of DEX CL in males compared with ovariectomized female rats with and without estradiol replacement therapy [39]. This may be attributed to the fact that Cyp3a2 is a male-specific isozyme in rats [40,41]. DEX plasma concentrations were captured well and our mPBPK model allows insights into tissue profiles by simulations to calculate the unbound ISF drug concentrations in controlling subsequent pharmacologic effects. A similar approach worked well for naproxen (NPX) in providing unbound ISF concentrations that corresponded well with direct measurements from other studies [42].

The PK was fixed when the PD model was used to capture DIS and drug effect parameters on paw edema in CIA rats. The physiological basis of the PD model was described in detail previously. The logistic function (k_g, Paw_{ss} *and* Paw) was used for natural growth of rats because of the existence of a plateau for rat growth. It is assumed that both paw edema due to CIA and natural growth contribute to the increased paw sizes, where paw edema was characterized by a turnover process with a first-order dissipation constant (k_{out}) and a zero-order rate constant ($k_{in}(t)$) which also declined with time (k_{deg}) accounting for the observed remission of paw swelling at later times. The T_{onset} parameter accommodates the delay between disease induction and the appearance of symptoms.

The present disease progression profiles in male and female CIA rats are consistent with previous observations from several studies [21,26,37]. However, model parameter estimates reveal both similarities and differences between the sexes. In terms of natural paw growth, females and males seem to have similar growth rates (similar kg rate constant estimates), although the initial paw sizes differ. Incorporation of IIV into initial paw sizes suggests that individual rats may have some variability because rats naturally differ in size. Interestingly, disease onset in female CIA rats occurs earlier than males, suggesting that female rats may have a more responsive immune system. This is consistent with the fact that there are more female RA patients and they have more reactive immune system [1,43]. Sex effects on disease production rate (k_{in}^0) were unexpectedly found not significant as determined by backward model parameter elimination, which differs from our previous study [26]. In addition, experimental observations indicated that female CIA rats developed arthritis faster and the symptoms were usually much more severe. One possible explanation could be the application of IIV on k_{in}^0, in the current model, which masks possible covariate effects. Another explanation could be that sex effects on k_{deg} may have an overlapping influence with k_{in}^0, in characterizing PD profiles. Interestingly, there is a sex difference in k_{deg}, which indicates that the underlying biological mechanism for disease progression may be different. Further studies of pro-inflammatory cytokines in male and female CIA rats may show different temporal profiles that may help to account for sex differences in k_{deg}. The time for peak edema is around day 16 for females and day 21 for males. The earlier peak time was also seen by others [24], suggesting that underlying inflammation starts earlier in female CIA rats and temporal profiles of pro-inflammatory processes may be inherently different between sexes. In our experiments, DEX administration substantially diminished the paw swelling within a very short time and the duration of drug effects lasted for two to three days after a single injection, which indicates that DEX is very potent in terms of immunosuppression. The I_{max} for the two sexes were equal to 1 indicating the ability of DEX to fully suppress paw edema while the IC_{50} value was greater in female rats. Although males appear more sensitive to DEX, clearance of DEX in males is greater leading to less exposure of DEX and so the overall drug effect in the two sexes is similar. The I_{max} estimates are comparable to results of previous modeling and *in vitro* assay [26]. For IC_{50}, there were less accurate estimates (larger %RSE) that may only serve as a rough indicator for comparing drug effects. Detailed mechanistic studies are needed to fill in this knowledge gap.

CONCLUSIONS

Effects of single doses of DEX (at two dose levels) in female and male CIA rats were well described by DIS and PK/PD models. A population approach allows statistical confirmation of sex differences in physiological and drug efficacy parameters based on the study design and large number of data points employed. The current DIS and response profiles can serve as a guide for design of further preclinical RA studies utilizing female CIA rats. Future studies quantifying pro-inflammatory biomarkers, such as IL-6 and other cytokines, in female paw tissues as was done in male rats [22,23] will allow the development of more mechanistic PK/PD/DIS models to explore sex differences in RA.

ACKNOWLEDGMENTS AND DISCLOSURES.

This work was supported by NIH Grant GM24211.

ABBREVIATIONS

AUC	Area under the curve
CS	Corticosteroids
CIA	Collagen-induced arthritis
DEX	Dexamethasone
DIS	Disease
GR	Glucocorticoid receptor
IIV	Inter-individual variability
IL	Interleukin
ISF	Interstitial fluid
mPBPK	Minimal physiologically-based pharmacokinetic
OFV	Objective function value
PD	Pharmacodynamics
PK	Pharmacokinetics
RA	Rheumatoid arthritis
SC	Subcutaneous

REFERENCES

1. Scott DL, Wolfe F, Huizinga TW. Rheumatoid arthritis. Lancet. 2010;376(9746):1094–108. [PubMed: 20870100]
2. Gaffo A, Saag KG, Curtis JR. Treatment of rheumatoid arthritis. Am J Health Syst Pharm. 2006;63(24):2451–65. [PubMed: 17158693]
3. Mateen S, Zafar A, Moin S, Khan AQ, Zubair S. Understanding the role of cytokines in the pathogenesis of rheumatoid arthritis. Clin Chim Acta. 2016;455:161–71. [PubMed: 26883280]
4. McInnes IB, Schett G. The pathogenesis of rheumatoid arthritis. N Engl J Med. 2011;365(23):2205–19. [PubMed: 22150039]
5. Brown PM, Pratt AG, Isaacs JD. Mechanism of action of methotrexate in rheumatoid arthritis, and the search for biomarkers. Nat Rev Rheumatol. 2016;12(12):731–42. [PubMed: 27784891]
6. Baschant U, Lane NE, Tuckermann J. The multiple facets of glucocorticoid action in rheumatoid arthritis. Nat Rev Rheumatol. 2012;8(11):645–55. [PubMed: 23045254]
7. Ronchetti S, Migliorati G. Riccardi C. GILZ as a mediator of the anti-inflammatory effects of glucocorticoids. Front Endocrinol (Lausanne). 2015;6:170. [PubMed: 26617572]
8. Losel R, Wehling M. Nongenomic actions of steroid hormones. Nat Rev Mol Cell Biol. 2003;4(1):46–56. [PubMed: 12511868]

9. Cato AC, Nestl A. Mink S. Rapid actions of steroid receptors in cellular signaling pathways. Sci STKE. 2002;2002(138):re9. [PubMed: 12084906]
10. Jawaheer D, Lum RF, Gregersen PK, Criswell LA. Influence of male sex on disease phenotype in familial rheumatoid arthritis. Arthritis Rheum. 2006;54(10):3087–94. [PubMed: 17009227]
11. Kovacs WJ, Olsen NJ. Sexual dimorphism of RA manifestations: genes, hormones and behavior. Nat Rev Rheumatol. 2011;7(5): 307–10. [PubMed: 21283144]
12. van Vollenhoven RF. Sex differences in rheumatoid arthritis: More than meets the eye. BMC Med. 2009;7:12. [PubMed: 19331649]
13. Danska JS. Sex matters for mechanism. Sci Transl Med 2014;6(258):258fs240.
14. Jorgensen TN. Sex disparities in the immune response. Cell Immunol. 2015;294(2):61–2. [PubMed: 25670393]
15. Lew KH, Ludwig EA, Milad MA, Donovan K, Middleton E Jr, Ferry JJ, et al. Gender-based effects on methylprednisolone pharmacokinetics and pharmacodynamics. Clin Pharmacol Ther. 1993;54(4):402–14. [PubMed: 8222483]
16. Kovats S. Estrogen receptors regulate innate immune cells and signaling pathways. Cell Immunol. 2015;294(2):63–9. [PubMed: 25682174]
17. Gubbels Bupp MR. Sex, the aging immune system, and chronic disease. Cell Immunol. 2015;294(2):102–10. [PubMed: 25700766]
18. Hegen M, Keith JC Jr, Collins M, Nickerson-Nutter CL. Utility of animal models for identification of potential therapeutics for rheumatoid arthritis. Ann Rheum Dis. 2008;67(11):1505–15. [PubMed: 18055474]
19. Bolon B, Stolina M, King C, Middleton S, Gasser J, Zack D, et al. Rodent preclinical models for developing novel antiarthritic molecules: comparative biology and preferred methods for evaluating efficacy. J Biomed Biotechnol. 2011;2011:569068. [PubMed: 21253435]
20. Moudgil KD, Kim P, Brahn E. Advances in rheumatoid arthritis animal models. Curr Rheumatol Rep. 2011;13(5):456–63. [PubMed: 21792748]
21. Earp JC, DuBois DC, Almon RR, Jusko WJ. Quantitative dynamic models of arthritis progression in the rat. Pharm Res. 2009;26(1): 196–203. [PubMed: 18758921]
22. Earp JC, DuBois DC, Molano DS, Pyszczynski NA, Almon RR, Jusko WJ. Modeling corticosteroid effects in a rat model of rheumatoid arthritis II: Mechanistic pharmacodynamic model for dexamethasone effects in Lewis rats with collagen-induced arthritis. J Pharmacol Exp Ther. 2008;326(2):546–54. [PubMed: 18448864]
23. Earp JC, DuBois DC, Molano DS, Pyszczynski NA, Keller CE, Almon RR, et al. Modeling corticosteroid effects in a rat model of rheumatoid arthritis I: Mechanistic disease progression model for the time course of collagen-induced arthritis in Lewis rats. J Pharmacol Exp Ther. 2008;326(2):532–45. [PubMed: 18448865]
24. Stolina M, Bolon B, Dwyer D, Middleton S, Duryea D, Kostenuik PJ, et al. The evolving systemic and local biomarker milieu at different stages of disease progression in rat collagen-induced arthritis. Biomarkers. 2008;13(7):692–712. [PubMed: 19096963]
25. Guo W, Yu D, Wang X, Luo C, Chen Y, Lei W, et al. Anti-inflammatory effects of interleukin-23 receptor cytokine-binding homology region rebalance T cell distribution in rodent collagen-induced arthritis. Oncotarget. 2016;7(22):31800–13. [PubMed: 27177334]
26. Li X, DuBois DC, Song D, Almon RR, Jusko WJ, Chen X. Modeling combined immunosuppressive and anti-inflammatory effects of dexamethasone and naproxen in rats predicts the steroid-sparing potential of naproxen. Drug Metab Dispos. 2017;45(7):834–45. [PubMed: 28416614]
27. Cao Y, Jusko WJ. Applications of minimal physiologically-based pharmacokinetic models. J Pharmacokinet Pharmacodyn. 2012;39(6):711–23. [PubMed: 23179857]
28. Samtani MN, Jusko WJ. Comparison of dexamethasone pharmacokinetics in female rats after intravenous and intramuscular administration. Biopharm Drug Dispos. 2005;26(3):85–91. [PubMed: 15654687]
29. Earp JC, Pyszczynski NA, Molano DS, Jusko WJ. Pharmacokinetics of dexamethasone in a rat model of rheumatoid arthritis. Biopharm Drug Dispos. 2008;29(6):366–72. [PubMed: 18613033]

30. McNamara PJ, Gibaldi M, Stoeckel K. Fraction unbound in interstitial fluid. J Pharm Sci. 1983;72(7):834–6. [PubMed: 6886999]
31. Post TM, Freijer JI, DeJongh J, Danhof M. Disease system analysis: basic disease progression models in degenerative disease. Pharm Res. 2005;22(7):1038–49. [PubMed: 16028004]
32. Dayneka NL, Garg V, Jusko WJ. Comparison of four basic models of indirect pharmacodynamic responses. J Pharmacokinet Biopharm. 1993;21(4):457–78. [PubMed: 8133465]
33. Beal SL, Sheiner LB, Boeckmann AL, Bauer RJ. NONMEM Users Guides, Icon Development Solutions, Ellicott City, MD, 2009.
34. Keizer RJ, Karlsson MO, Hooker A. Modeling and simulation workbench for NONMEM: Tutorial on Pirana, PsN, and Xpose. CPT Pharmacometrics Syst Pharmacol. 2013;2:e50. [PubMed: 23836189]
35. Lindbom L, Pihlgren P, Jonsson EN. PsN-Toolkit–a collection of computer intensive statistical methods for non-linear mixed effect modeling using NONMEM. Comput Methods Prog Biomed. 2005;79(3):241–57.
36. R-Core Team. R: a language and environment for statistical computing. Vienna: Foundation for Statistical Computing; 2008.
37. Lon HK, Liu D, DuBois DC, Almon RR, Jusko WJ. Modeling pharmacokinetics/pharmacodynamics of abatacept and disease progression in collagen-induced arthritic rats: a population approach. J Pharmacokinet Pharmacodyn. 2013;40(6):701–12. [PubMed: 24233383]
38. Tomlinson ES, Maggs JL, Park BK, Back DJ. Dexamethasone metabolism in vitro: species differences. J Steroid Biochem Mol Biol. 1997;62(4):345–52. [PubMed: 9408089]
39. Lamiable D, Vistelle R, Fay R, Bensussan B, Millart H, Wiczewski M, et al. Influence of sex and oestrogen replacement on the disposition of dexamethasone in rats. Fundam Clin Pharmacol. 1991;5(8):733–40. [PubMed: 1783362]
40. Kato R, Yamazoe Y. Sex-specific cytochrome P450 as a cause of sex- and species-related differences in drug toxicity. Toxicol Lett. 1992;64–65 Spec No:661–667.
41. Maggs JL, Morgan P, Park BK. The sexually differentiated metabolism of [6,7–3H]17 beta-oestradiol in rats: male-specific 15 alpha-and male-selective 16 alpha-hydroxylation and female-selective catechol formation. J Steroid Biochem Mol Biol. 1992;42(1):65–76. [PubMed: 1313694]
42. Li X, DuBois DC, Almon RR, Jusko WJ. Modeling sex differences in pharmacokinetics, pharmacodynamics, and disease progression effects of naproxen in rats with collagen-induced arthritis. Drug Metab Dispos. 2017;45(5):484–91. [PubMed: 28246127]
43. Cutolo M, Villaggio B, Seriolo B, Montagna P, Capellino S, Straub RH, et al. Synovial fluid estrogens in rheumatoid arthritis. Autoimmun Rev. 2004;3(3):193–8. [PubMed: 15110231]
44. Shah DK, Betts AM. Towards a platform PBPK model to characterize the plasma and tissue disposition of monoclonal antibodies in preclinical species and human. J Pharmacokinet Pharmacodyn. 2012;39(1):67–86. [PubMed: 22143261]

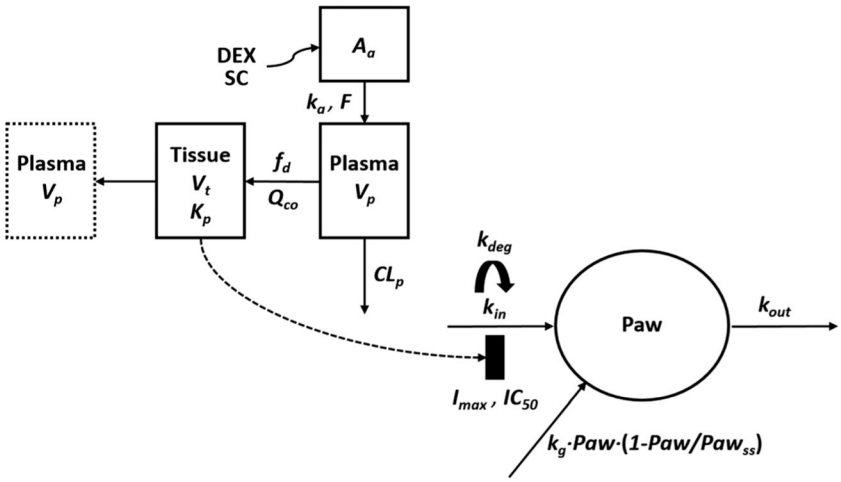

Fig. 1.

Schematic of the PK/PD/DIS progression model for effects of DEX on paw edema in CIA rats. Parameters are defined in the text and in Tables I and II.

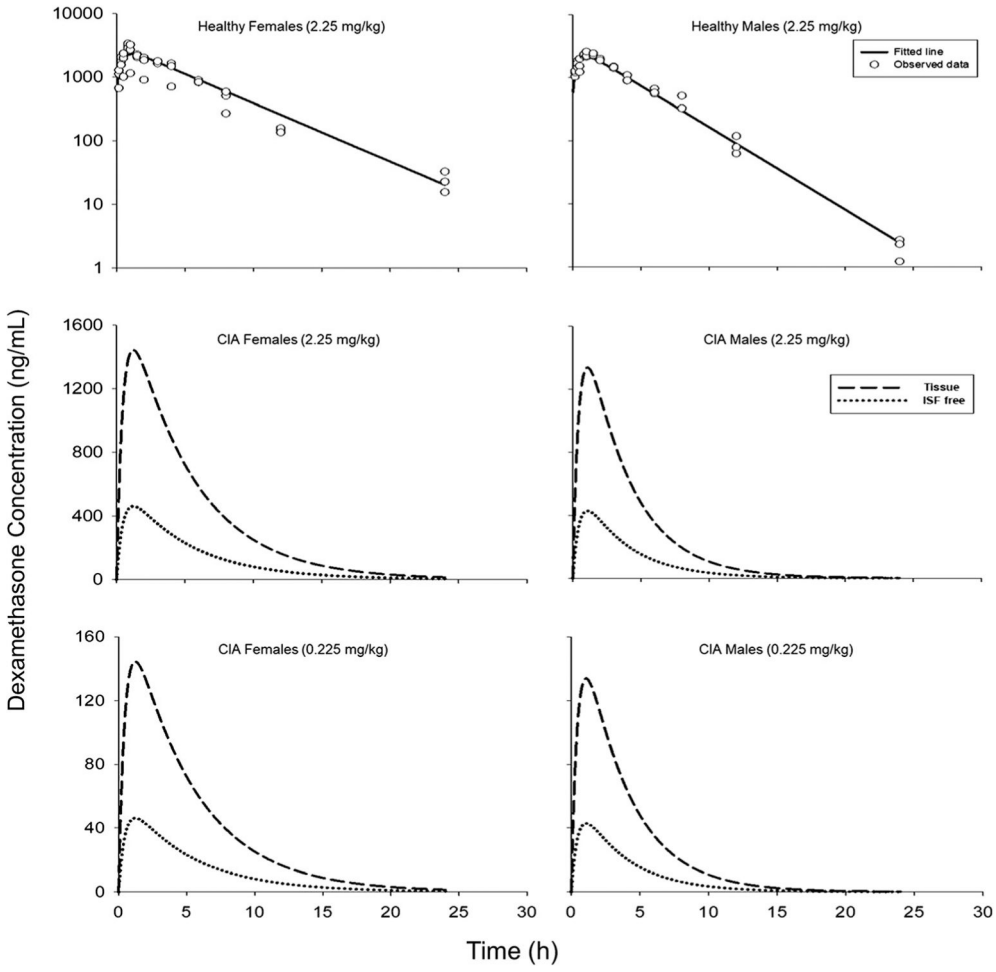

Fig. 2.

Upper panel: PK model fitting of DEX plasma profiles in healthy female and male rats that received 2.25 mg/kg doses (Solid lines: model predictions; dots: observed data). Middle and lower panel: Simulated total tissue (dashed lines) and unbound ISF concentrations (dotted lines) of DEX in female and male arthritic rats that received 0.225 or 2.25 mg/kg SC DEX based on the PK model in Fig. 1 and parameters listed in Table I.

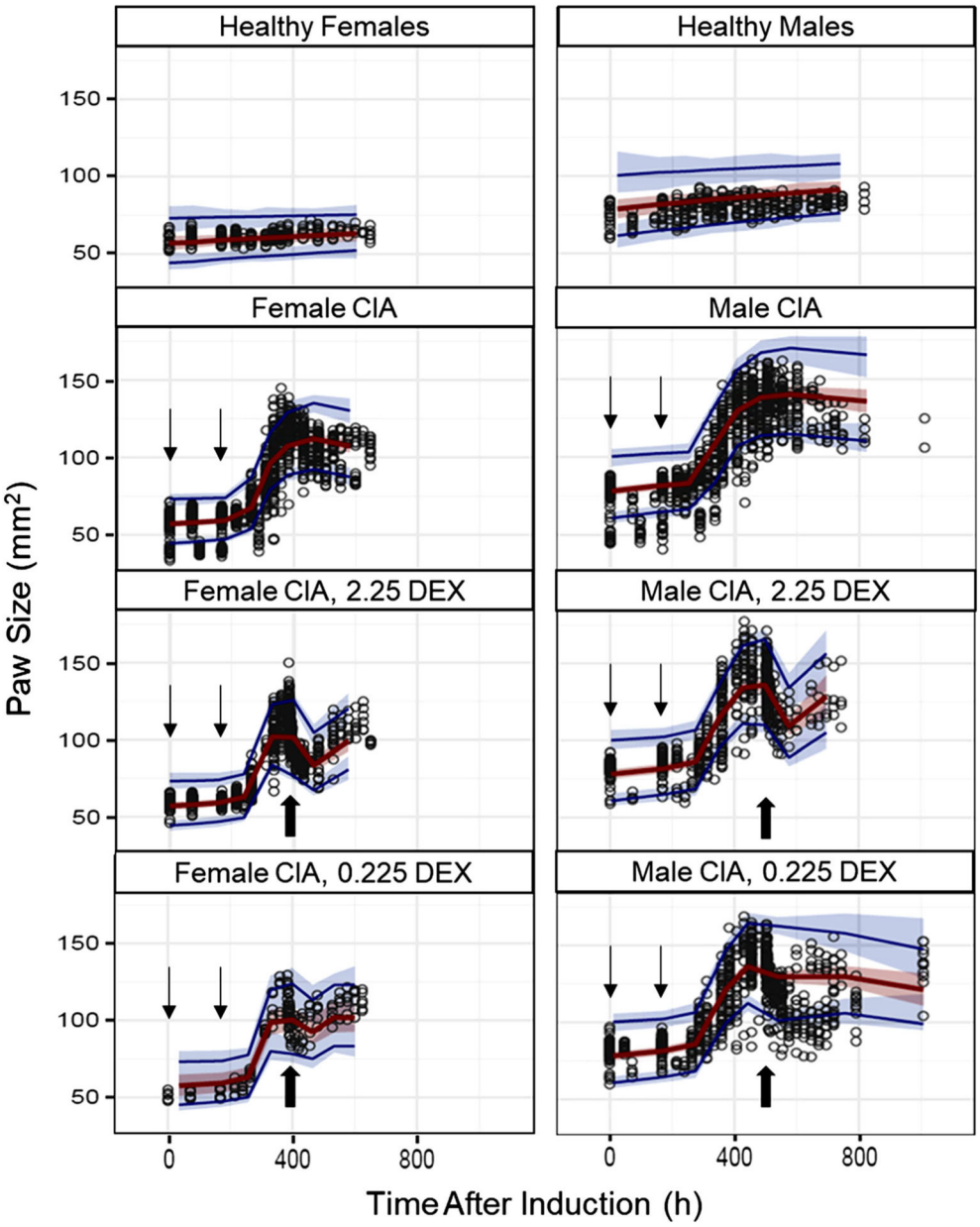

Fig. 3.

Paw size values and mode fittings shown as VPC plots. The 95th, median, and 5th percentiles of predicted paw sizes are represented by upper blue lines, red lines and lower blue lines. The red-shaded area depicts the 95% confidence interval for the median predictions, whereas the upper and lower blue-shaded areas depict the 95% confidence intervals for the 95th and 5th percentiles of predicted concentrations. Disease induction on days 0 and 7 are marked by line arrows and DEX dosing for females (day 16) and males (day 21) are indicated by block arrows.

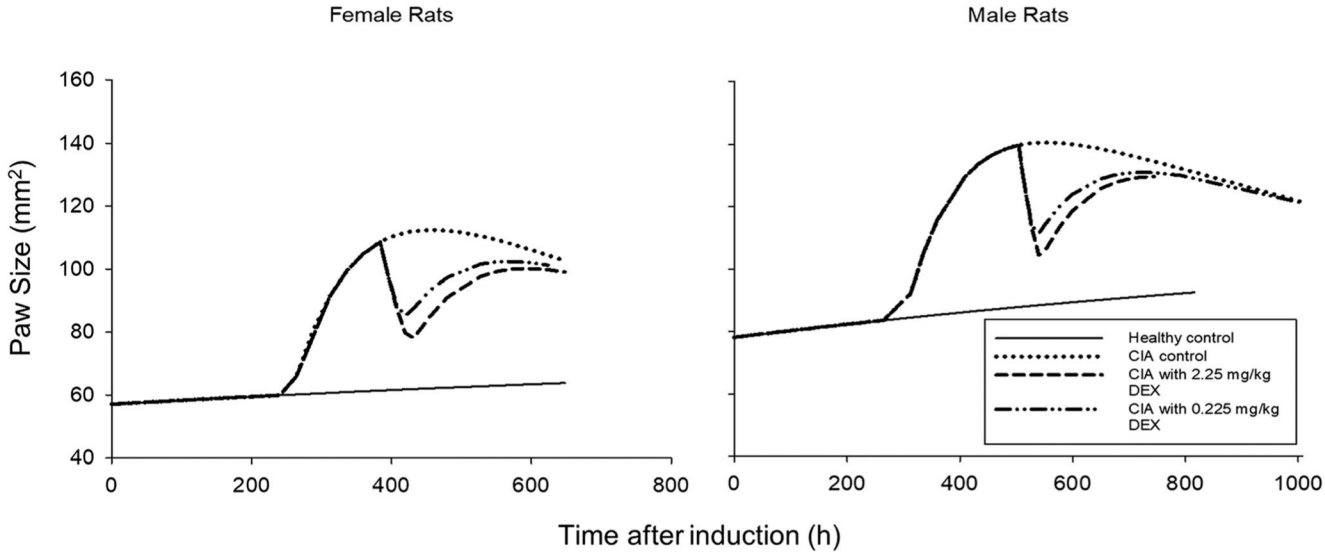

Fig. 4.

Population prediction profiles of paw edema measurements versus time for female and male rats. Insert indicates sex and treatment groups.

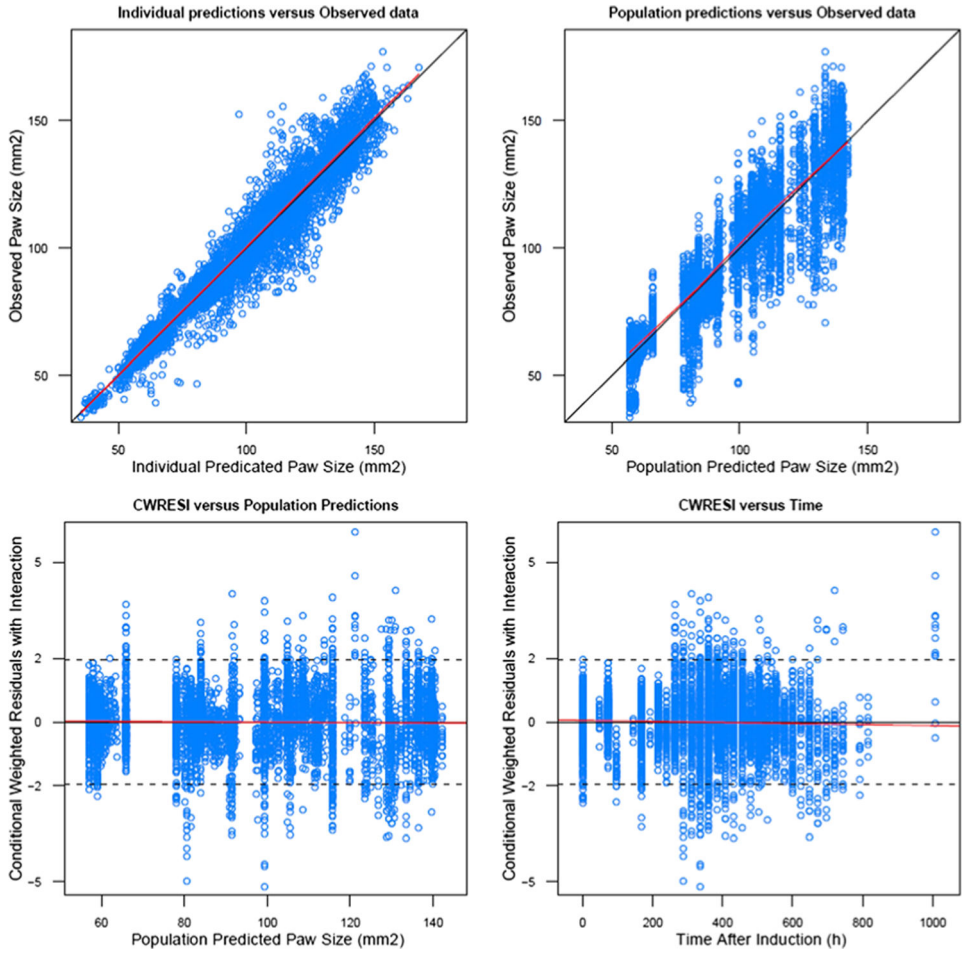

Fig. 5.

Goodness-of-fit plots of DEX PD model in CIA rats showing individual model predictions versus observed paw edema (upper left); population model predictions versus observed paw edema values (upper right); conditional weighted residuals with interaction versus population predictions (lower left); conditional weighted residuals with interaction versus time after induction. Lines are the identity lines for upper panels and zero slope lines for lower panels.

Table I

Pharmacokinetic Parameter Values for DEX

Parameter (units)	Definition	Estimates
k_a (1/h)	Absorption rate constant of DEX	2.09 [b]
f_d	Fraction of cardiac plasma flow of DEX	1 [b]
$CL_{p\ Females}$ (mL/h/kg)	Clearance of DEX in female rats	137.8 [b]
$CL_{p\ Males}$ (mL/h/kg)	Clearance of DEX in male rats	197.7 [b]
K_p	Tissue partition coefficient of DEX	0.63 [b]
V_p (mL/kg)	Plasma volume	32.36 [a]
V_t (mL/kg)	Tissue volume	967.6 [a]
Q_{co} (mL/h/kg)	Cardiac plasma flow	7650 [a]

[a] Physiological parameter values obtained from Ref (44)

[b] PK parameter values of DEX obtained from Ref (26)

Table II

Pharmacodynamic Parameter Estimates for DEX Efficacy for Paw Edema in CIA Rats

Parameters (units)	Definition	Females		Males	
		Estimate (%RSE)	IIV (%RSE)	Estimate (%RSE)	IIV (%RSE)
Disease-specific					
t_{onset} (h)	Time of disease onset	256 (0.4)	NA	300 (0.6)	NA
k_{out} (1/h)	Loss of edema rate constant	0.0088 (8.2)	NA	0.0088 (8.2)	NA
k_{deg} (1/h)	Loss of production rate constant	0.00099 (8.4)	NA	0.00047 (18.1)	NA
k_g (1/h)	Natural growth rate constant	0.00101 (20.4)	NA	0.00101 (20.4)	NA
Paw_{ss} (mm^2)	Paw size at steady-state	73.1 (5.3)	NA	108 (7.4)	NA
Paw_0 (mm^2)	Paw size on day 0	57.1 (1.0)	13.2 (6.3)	78.1 (0.8)	13.2 (6.3)
k_{in}^0 (mm^2/h)	Disease production rate constant at t_{onset}	1.66 (4.8)	10.7 (4.3)	1.66 (4.8)	10.7 (4.3)
ε (%)	RV (prop)	0.59 (6.3)		0.59 (6.3)	
Drug-specific					
I_{max}	Maximum inhibition	1 (Fixed)	NA	1 (Fixed)	NA
IC_{50} (ng/mL)	Unbound ISF DEX concentration at 50% I_{max}	0.101 (60.4)	NA	0.0146 (135.6)	NA